

Electronic Supplementary Information (ESI) Available

Thermal Shock Initiated Thermal and Chemical Responses of HMX Crystal from ReaxFF Molecular Dynamics Simulation

(Tingting Zhou, Huajie Song, Yi Liu, Fenglei Huang)

Table S1 Stress tensors for the systems after uniaxial compression obtained from NVT-MD (unit: GPa)

compression	P	P_{xx}	P_{yy}	P_{zz}	P_{xy}	P_{xz}	P_{yz}
0	0.0003	0.2551	-0.1159	-0.1382	-0.0207	0.2283	0.0061
15%	9.4243	8.3010	10.9521	9.0199	-0.1721	0.0156	0.3375
30%	43.2251	42.7550	46.0505	40.8698	0.6204	-0.4045	0.1971

Table S2. Bond order cutoff values for various atom pairs. The algorithm of molecule recognition in the fragment analysis uses these values.

	C	H	O	N
C	0.55	0.40	0.60	0.30
H		0.55	0.40	0.55
O			0.65	0.40
N				0.55

Table S3. Comparisons of important physical parameters under thermal shock for HMX crystals with 0, 15 %, and 30 % compression

ΔV (%)	t_p (ps)	t_d (ps)	V_s ($\text{km}\cdot\text{s}^{-1}$)	V_{p_max} ($\text{km}\cdot\text{s}^{-1}$)	κ ($\text{W}\cdot\text{m}^{-1}\cdot\text{K}^{-1}$)	T_{RF} (K)	T_{RC} (K)	V_{RF} ($\text{km}\cdot\text{s}^{-1}$)	V_{RC} ($\text{km}\cdot\text{s}^{-1}$)
0	4	20	3.32	0.5	0.80	1080	1780	0.069	0.038
15	2	14	5.67	0.26	1.25	1550	2100	0.094	0.063
30	< 1	5	> 9.33	0.16	1.82	1780	2280	0.155	0.108

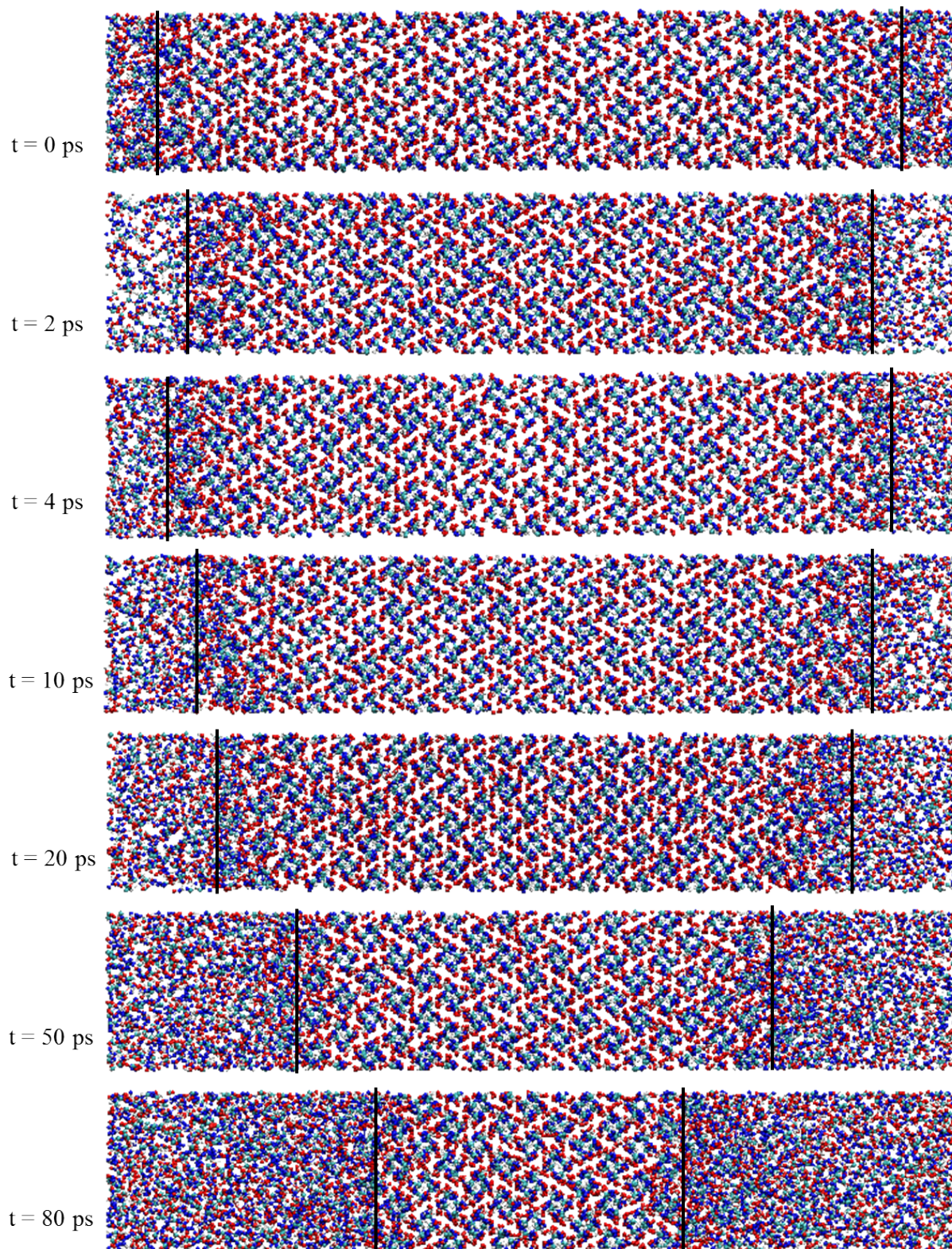


Figure S1. Microstructure profile for HMX crystal ($\Delta V = 0$) at various times under thermal shock. The region between the two vertical lines has HMX crystalline structure, while the rest of system is amorphous due to thermal decomposition.

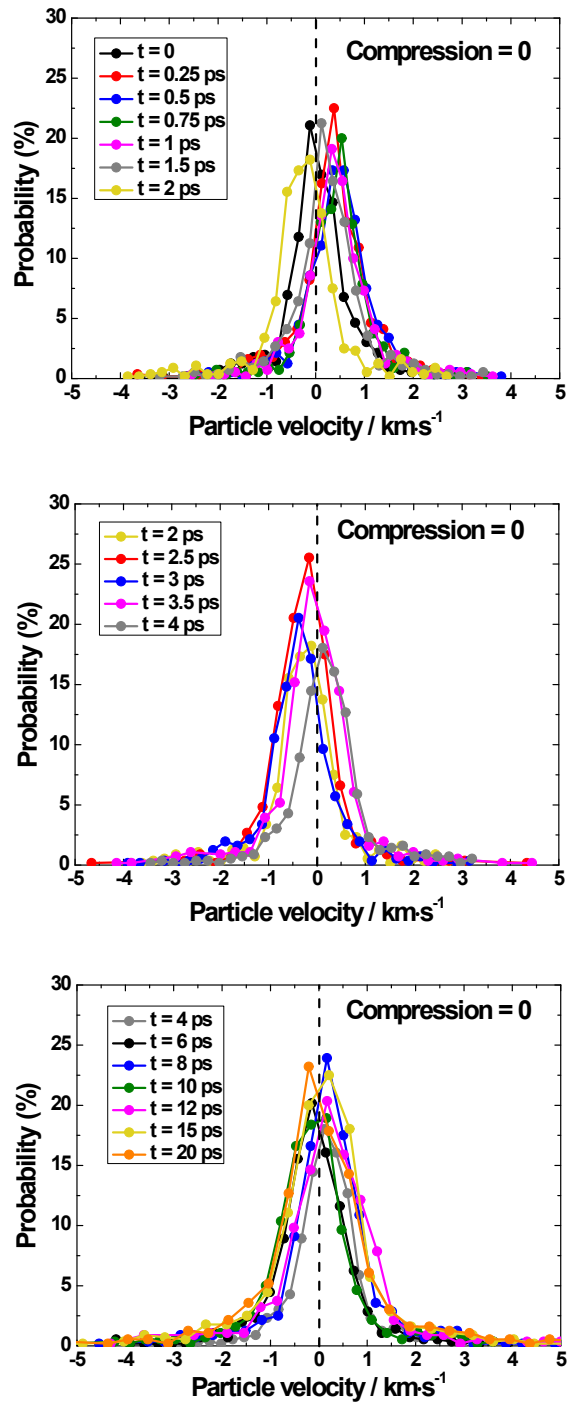


Figure S2. Probability distribution of particle velocity under thermal shock for HMX crystal without compression. Particles move in the same direction of heat propagation at $t < 2$ ps and move in the opposite direction at $2 < t < 4$ ps.

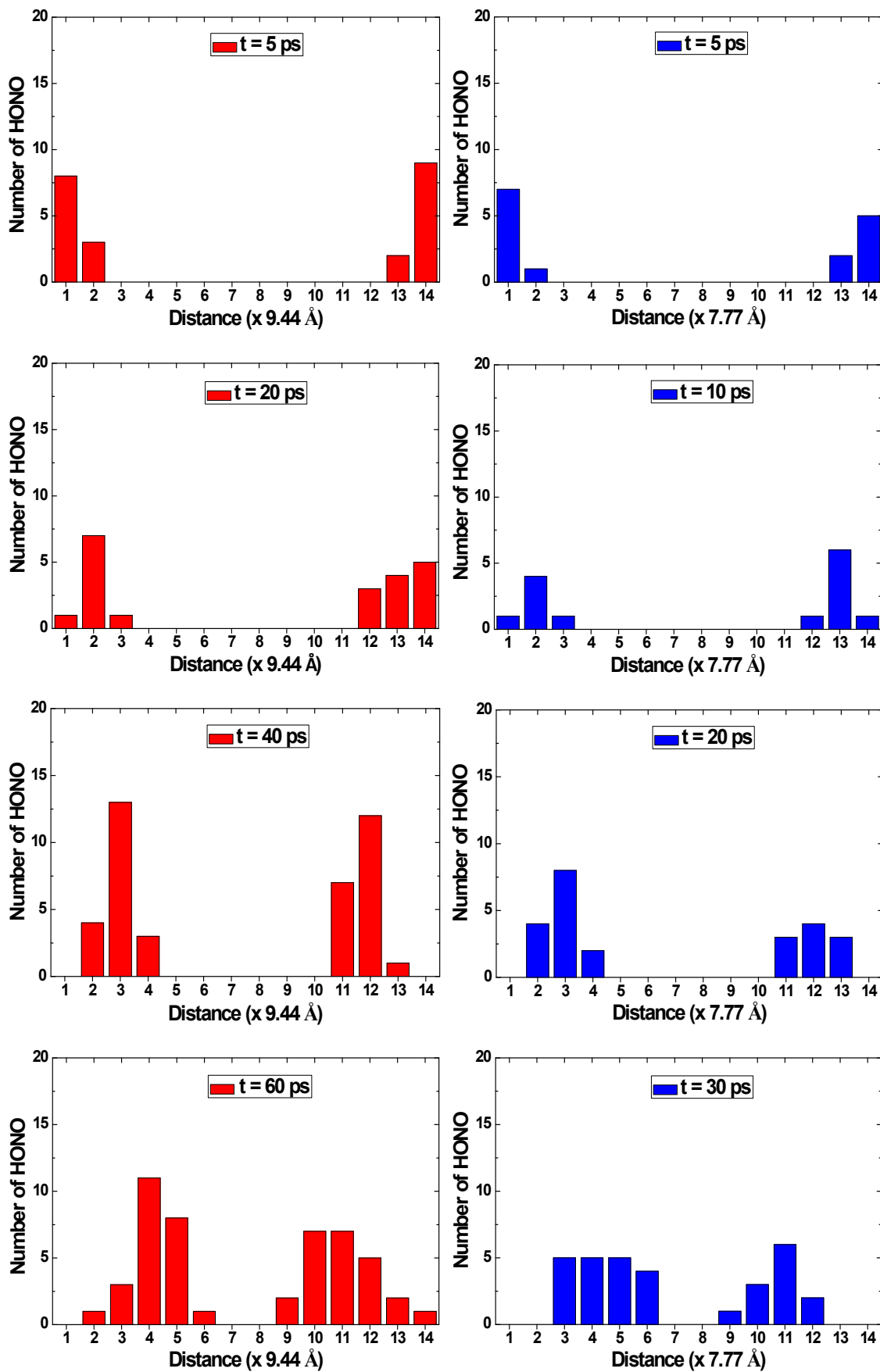


Figure S3. Spatial distributions of HONO at various times under thermal shock for HMX crystals with 15 % compression (left) and with 30 % compression (right)

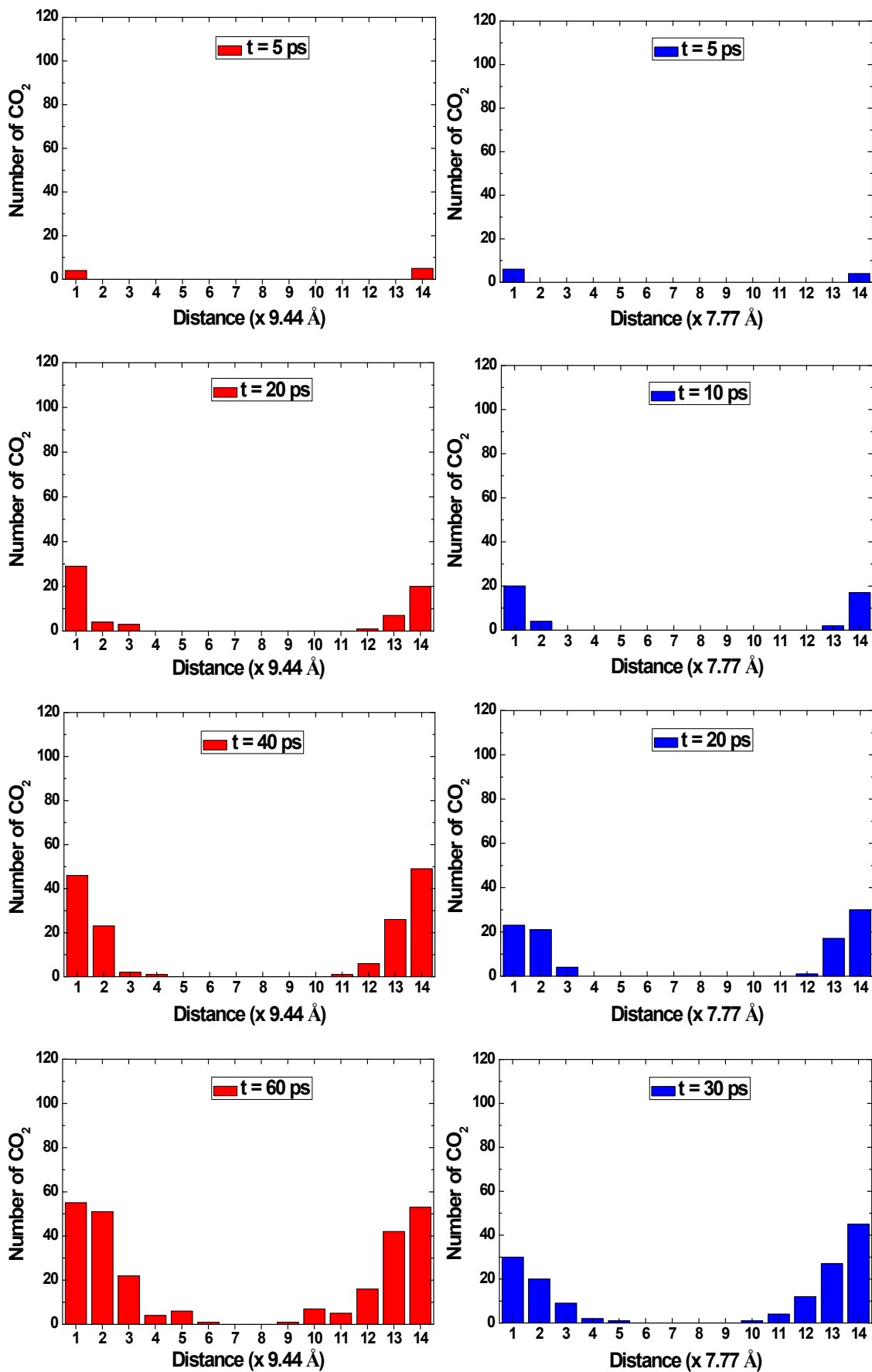


Figure S4. Spatial distributions of CO₂ at various times under thermal shock for HMX crystals with 15 % compression (left) and with 30 % compression (right)

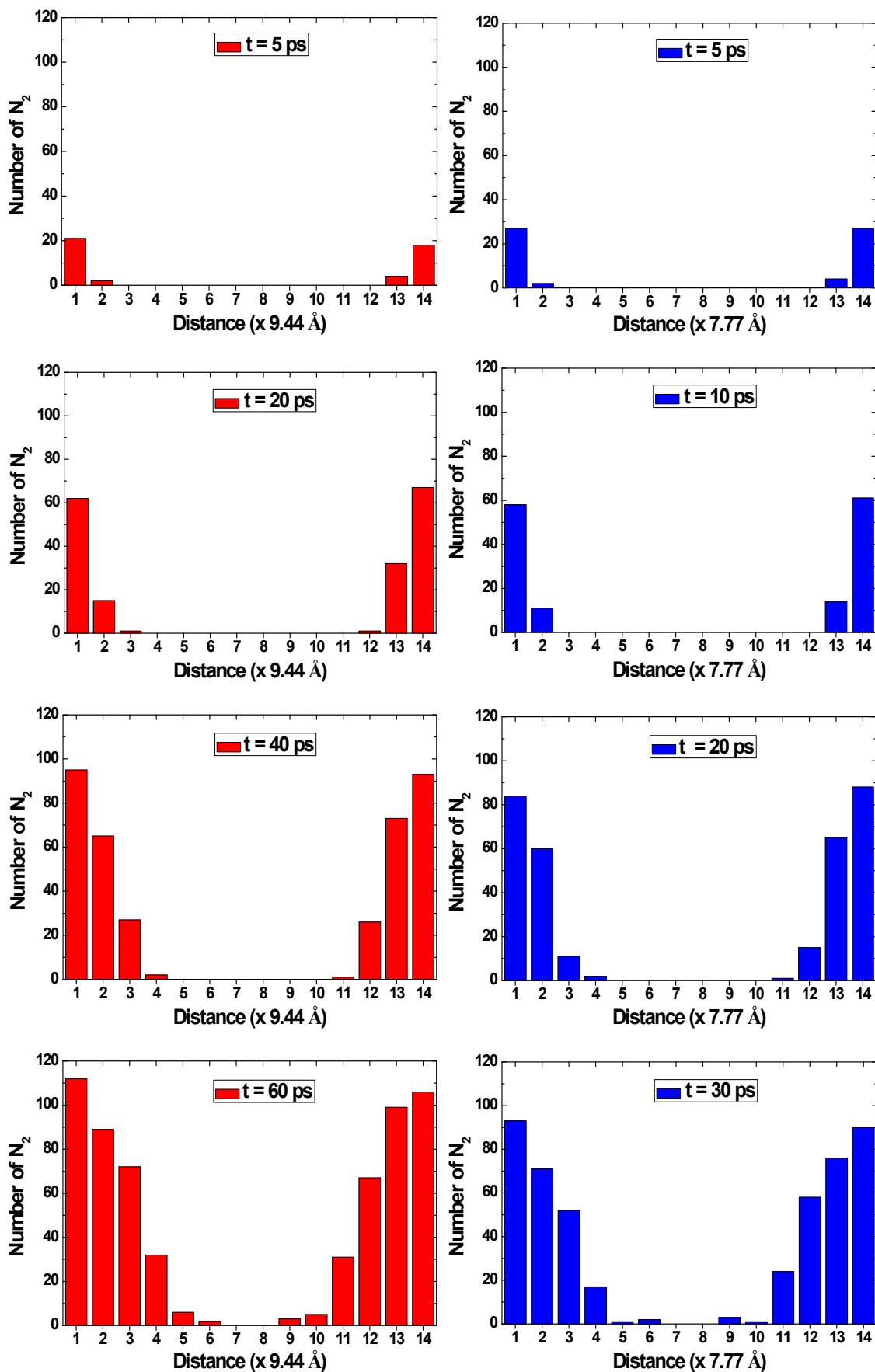


Figure S5. Spatial distributions of N_2 at various times under thermal shock for HMX crystals with 15 % compression (left) and with 30 % compression (right)

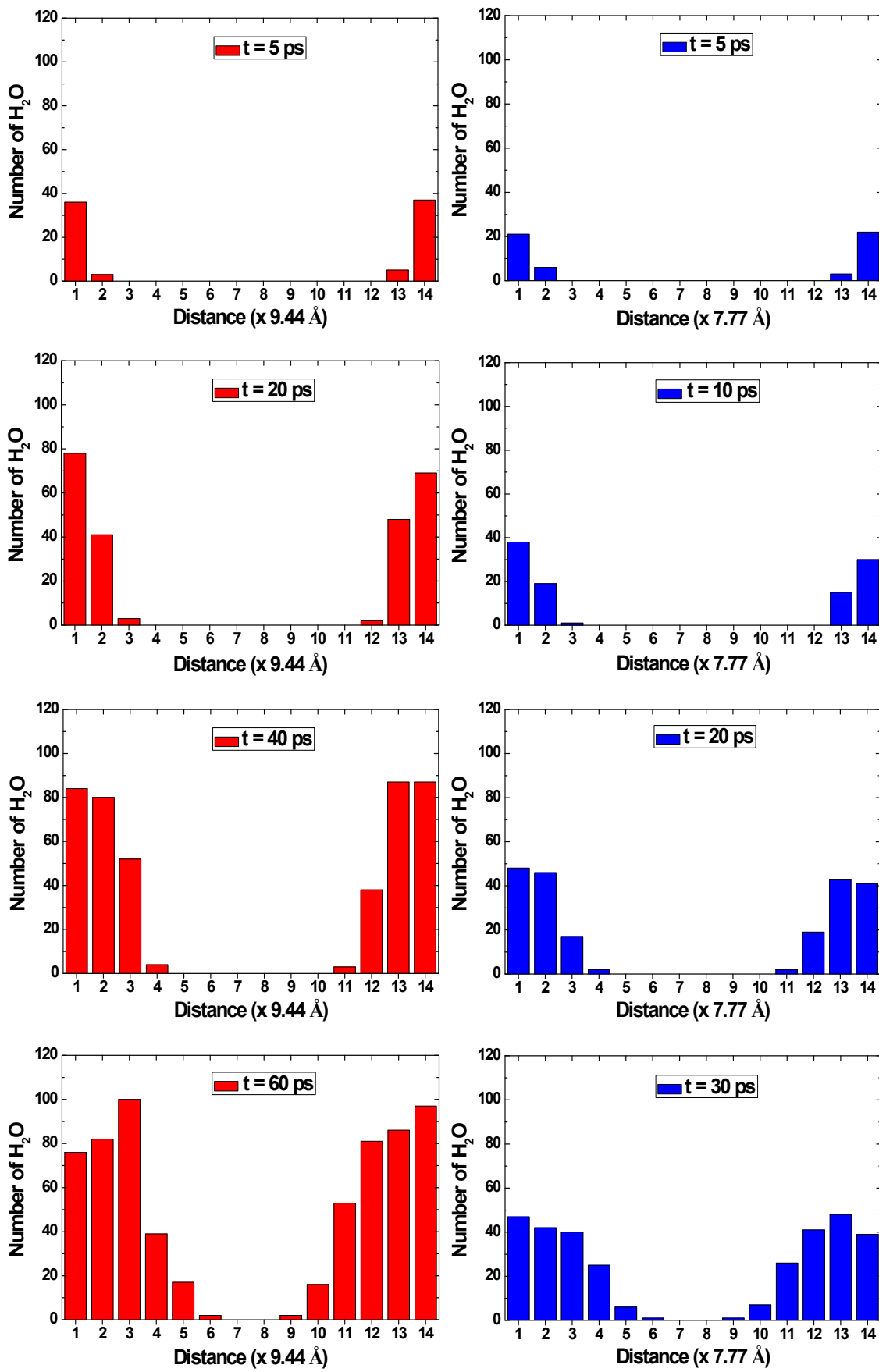


Figure S6. Spatial distributions of H₂O at various times under thermal shock for HMX crystals with 15 % compression (left) and with 30 % compression (right)